

doi: 10.12029/gc20160606

马士委, 周志广, 柳长峰, 等. 内蒙古西乌旗地区晚石炭世石英闪长岩的岩石成因及构造意义[J]. 中国地质, 2016, 43(6): 1932–1946.

Ma Shiwei, Zhou Zhiguang, Liu Changfeng, et al. Petrogenesis and Tectonic significance of the Late Carboniferous quartz diorite in Xi Ujimqin Banner, Inner Mongolia [J]. *Geology in China*, 2016, 43(6): 1932–1946(in Chinese with English abstract).

内蒙古西乌旗地区晚石炭世石英闪长岩的岩石成因 及构造意义

马士委¹ 周志广² 柳长峰² 李瑞杰³ 来 林⁴ 张学斌⁴ 孟元库⁵

(1. 中国地质科学院地质研究所, 中国地质调查局大陆动力学研究中心, 北京 100037; 2. 中国地质大学地球科学与资源学院, 北京 100083; 3. 北京市地质调查研究院, 北京 102206; 4. 天津市地质调查研究院, 天津 300191; 5. 中国地质调查局青岛海洋地质研究所, 山东 青岛 266071)

摘要: 内蒙古西乌旗地区出露一些石英闪长岩, 其 LA-ICP-MS 锆石 U-Pb 年龄为 (304.64 ± 0.82) Ma 和 (309.84 ± 0.86) Ma, 表明这套岩石形成于晚石炭世。地球化学分析表明, 西乌旗地区石英闪长岩属于低 TiO_2 和高 Al_2O_3 钙碱性玄武岩系列; 富集 Rb、Ba、K 大离子亲石元素 (LILE), 亏损 Nb、Ta、Ti、P 等高场强元素 (HFSE), 具有典型弧岩浆岩的特征, 显示岩浆源区曾经历过俯冲带流体的交代作用; 稀土元素丰度偏低, 呈 LREE 富集 HREE 亏损的右倾模式; 强不相容元素比值 (La/Nb、La/Ta 等) 及判别图解表明晚石炭世石英闪长岩类似大陆边缘弧玄武岩, 岩浆来源于浅部岩石圈地幔, 系石榴石+尖晶石二辉橄榄岩源区中等程度 (10%~20%) 部分熔融的结果。综合研究区样品的地球化学特征, 结合区域地质资料及对比分析前人成果, 认为早石炭世末期西乌旗地区在强烈拉张的裂谷环境下形成了有限洋盆, 由于洋盆发育不成熟或边伸展边向两侧俯冲—消减, 形成了西乌旗地区类似大陆边缘弧玄武岩特征的晚石炭世石英闪长岩。

关键词: 石英闪长岩; 锆石年龄; 地球化学; 拉张环境, 晚石炭世; 西乌旗

中图分类号: P588.12² 文献标志码: A 文章编号: 1000-3657(2016)06-1932-15

Petrogenesis and tectonic significance of Late Carboniferous quartz diorite in Xi Ujimqin Banner, Inner Mongolia

MA Shi-wei¹, ZHOU Zhi-guang², LIU Chang-feng², LI Rui-jie³,
LAI Lin⁴, ZHANG Xue-bin⁴, MENG Yuan-ku⁵

(1. *Institute of Geology, Chinese Academy of Geological Sciences, Center for Continental Dynamics, CGS, Beijing 100037, China;*
2. *School of Earth Sciences and Resources, China University of Geosciences, Beijing 100083, China;* 3. *Beijing Institute of Geological Survey, Beijing 102206, China;* 4. *Tianjin Institute of Geological Survey, Tianjin 300191, China;* 5. *Qingdao Institute of Marine Geology, China Geological Survey, Qingdao, Shandong, 266071*)

收稿日期: 2015-08-27; 改回日期: 2016-01-14

基金项目: 国家自然科学基金委创新群体项目 (40921001)、国土资源部公益性行业基金项目 (201511022、201211093)、中国地质调查局项目 (12120115026801、1212011120700、1212011220465、12120114093901) 联合资助。

作者简介: 马士委, 男, 1986 年生, 博士生, 构造地质学专业, 主要从事岩石大地构造与构造成矿; E-mail: mswei1986@163.com。

通讯作者: 孟元库, 男, 1986 年生, 主要从事岩石大地构造和海洋地质调查; E-mail: ykmeng@foxmail.com。

Abstract: Late Carboniferous quartz diorites are distributed in the Xi Ujimqin Banner of Inner Mongolia. The results of LA-ICP-MS zircon U-Pb dating of the quartz diorite samples indicate ages of 304.64 ± 0.82 Ma and 309.84 ± 0.86 Ma. In addition, new geochemical data from six quartz diorite samples are presented. All six samples show high Al_2O_3 values but low TiO_2 values, and are thus classified as calc-alkali basalt series. These samples are characterized by low REE abundance and slight LREE enrichment. They also show LILE enrichment, HFSE depletion and distinctly negative Nb and Ta anomalies. All of these characteristics resemble those of arc magmatic rocks. Furthermore, as shown in the correlation plots of La/Ba versus La/Nb, Ba/La versus Ce/Pb, and Nb/Y versus La/Yb, the magma source has experienced contamination and metasomatism from the subduction fluid. According to the Zr/Nb, La/Nb, La/Ta ratios and the diagram of Sm/Yb versus La/Sm, the magma was derived from the shallow lithospheric mantle and formed by moderate (10%–20%) partial melting of spinel-garnet lherzolites. Based on geochemical characteristics of these samples in this study, combined with regional geological data and previous research results, the authors hold that, in the late Early-Carboniferous, there was a new limited ocean basin under an intensely extensional rift setting. Consequently, as the newly formed ocean basin was still immature or experienced subduction-related contamination and metasomatism, the Late Carboniferous quartz diorites of Xi Ujimqin Banner exhibited the continental margin-arc-like enriched signatures.

Key words: quartz diorite; zircon U-Pb dating; geochemistry; extensional setting; late Carboniferous; Xi Ujimqin Banner

About the first author: MA Shi-wei, male, born in 1986, doctor candidate, majors in structural geology, mainly engages in the study of petro-tectonics and mineralization; E-mail: mswei1986@163.com.

Fund support: Supported by the National Science Foundation of China (No. 49021001), Public Welfare Profession Foundation of Ministry of Land and Resources (No. 201511022, 201211093) and Project of Geological Survey of China (No. 12120115026801, 1212011120700, 1212011220465, 12120114093901).

中亚造山带是全球显生宙地壳增生与改造最显著的地区,其构造演化一直备受国内外学者的关注与研究,详细的增生过程仍然是国际学术界争议的前沿课题^[1-10]。中国内蒙古地区位于中亚造山带中东部,华北板块与西伯利亚板块之间,区内岩浆活动频繁,岩浆弧和增生楔中散布着众多前寒武纪微地块和条带状蛇绿岩,正确认识各地质体间的时空关系对解决中亚造山带的构造演化具有重要意义^[11]。长期以来,在内蒙古地区晚古生代构造演化的问题上一值存在争议,焦点之一就是该地区古亚洲洋的最终闭合时间。关于古亚洲洋的闭合时间,存在多种不同的观点:泥盆纪^[7-8,12]、石炭纪早期^[9,13]、二叠纪^[1,3-4,14-18]。

内蒙古西乌旗位于内蒙古中部即兴蒙造山带范围内,西乌旗地区广泛出露晚石炭世石英闪长岩,储存了大量晚古生代构造演化信息,但对该地区石炭纪的构造环境仍存在争议。鲍庆中等^[19]对西乌旗白音高勒地区的石炭纪石英闪长岩进行了SHRIMP锆石U-Pb年代学测定,所获年龄为 $(313 \pm 5)Ma \sim (323 \pm 4)Ma$,认为其形成于华北板块与亲西伯利亚板块碰撞之后的张性构造环境。刘建峰等^[11]通过分析西乌旗南部的石炭纪石英闪长岩的地球

化学特征,认为其形成于与俯冲有关的活动陆缘的构造环境,并且获得了 $(325 \pm 3)Ma$ 和 $(323 \pm 3)Ma$ 两个LA-ICP-MS锆石U-Pb年龄。因此本文在1:5万区域地质调查的基础上,选择西乌旗南部猴头庙出露的石英闪长岩(图1-a)进行岩石学、年代学和地球化学研究,探讨其形成的构造环境,以期为该地区的晚古生代构造演化提供新的依据。

1 地质概况及岩石特征

研究区位于内蒙古西乌旗南部,大地构造位置上处于西伯利亚板块南缘增生带与华北板块北缘增生带的碰撞接壤部位,同时也位于贺根山蛇绿岩带和温都尔庙-西拉木伦河缝合带之间(图1-b)。区内晚古生代岩浆活动强烈,研究区石英闪长岩以岩滴和小岩基形式产出,其侵入到早元古代宝音图群、奥陶纪布龙山组、石炭系本巴图组和早石炭世闪长岩,部分岩体还带有片岩捕虏体,并且石英闪长岩被二叠纪花岗岩侵入,出露面积约 $20 km^2$ 。少数岩石发生韧性变形,局部岩石见有闪长质暗色包体(图2-a、b)。岩石呈浅灰色、灰白色、浅灰绿色,中细粒半自形柱状结构,块状构造。主要由斜长石、角闪石和石英组成。镜下特征为:斜长石1~3

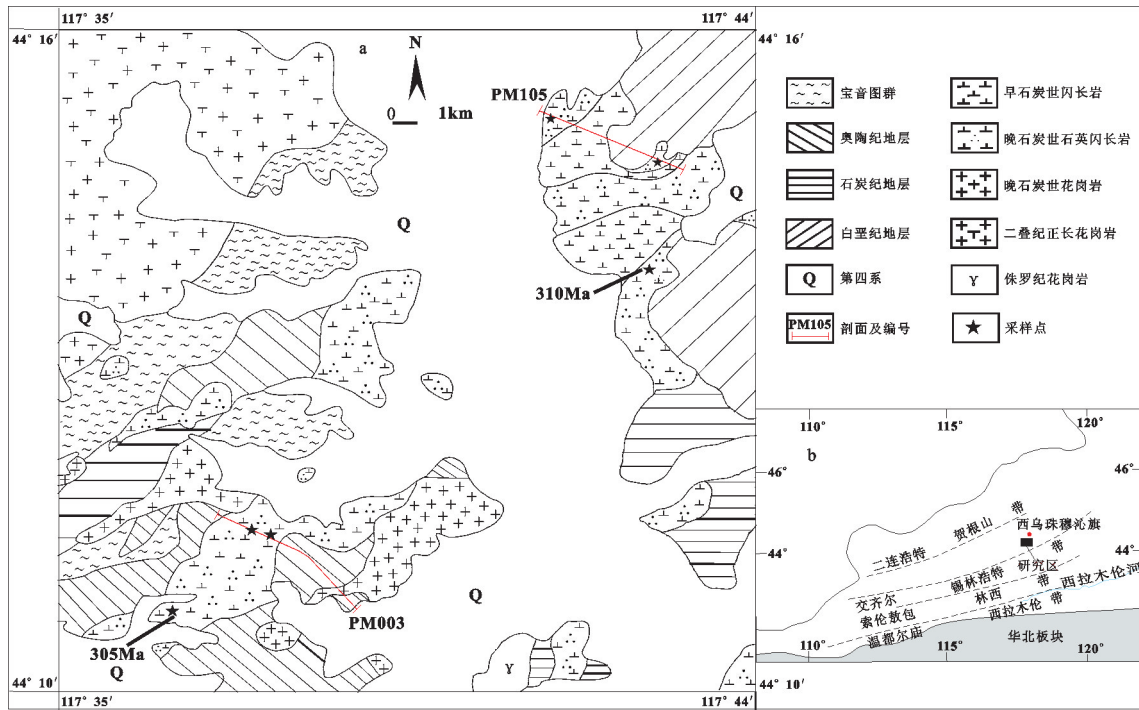


图1 研究区地质简图和大地构造位置简图

a—研究区地质简图,据资料①修改;b—大地构造位置简图,据[4]和[17]修改

Fig. 1 Geological sketch map and simplified tectonic geological map

a—Geological sketch map (modified after reference ①);

b—Simplified tectonic geological map (modified after references [4] and [17])

mm,半自形板状,发育聚片双晶,绢云母化、黝帘石化,含量约45%~55%;浅黄—褐色角闪石1~2 mm,长柱状,部分绿泥石化、次闪石化,与斜长石相间分布,韧性变形的岩石角闪石被挤压呈透镜状长轴定向排列,含量约30%~35%;石英他形细粒状,分布在斜长石和角闪石之间,含量约10%~15%;黑云母少量;岩石中见有磁铁矿、榍石、磷灰石等副矿物(图2-c、d)。本文采集了6个比较新鲜的地球化学样品和2个比较新鲜的年龄样品,采样位置见图1-a。

2 样品分析方法

样品主量元素和微量元素在河北省区域地质矿产调查研究所实验室分别采用XRF和ICP-MS仪器完成,主量元素相对标准偏差(RSD)小于5%,微量元素的RSD小于10%。

锆石的挑选由河北省区域地质矿产调查研究

所实验室完成,制靶和阴极发光实验在北京锆年领航科技有限公司制备,锆石U-Pb年龄在天津地质调查中心激光剥蚀等离子体质谱仪(LA-ICP-MS)上测定,具体实验原理和数据处理方法详见参考文献[20]。

3 年代学特征

本文对研究区出露的石英闪长岩进行了LA-ICP-MS锆石U-Pb年代学研究。所选样品阴极发光图像(CL)如图3所示,U-Pb谐合图见图4,LA-ICP-MS锆石U-Pb年龄结果见表1。

样品D3014-TW1采样位置为东经117°35'58",北纬44°10'46",D3021-TW1采样位置为东经117°41'53",北纬44°14'02"。锆石浅褐色到黑色,晶形复杂,短柱状和粒状,少数长柱状。从阴极发光图像(图3)中可以看出,大部分锆石韵律环带比较发育,

①中国地质大学(北京)地质调查研究院.内蒙古1:5万巴拉格勒农业分场幅(L50E022015)、阿拉腾格勒公社幅(L50E022016)、猴头庙幅(L50E023015)、阿拉腾包大队幅(L50E023016)区域地质调查报告[R]. 2012.

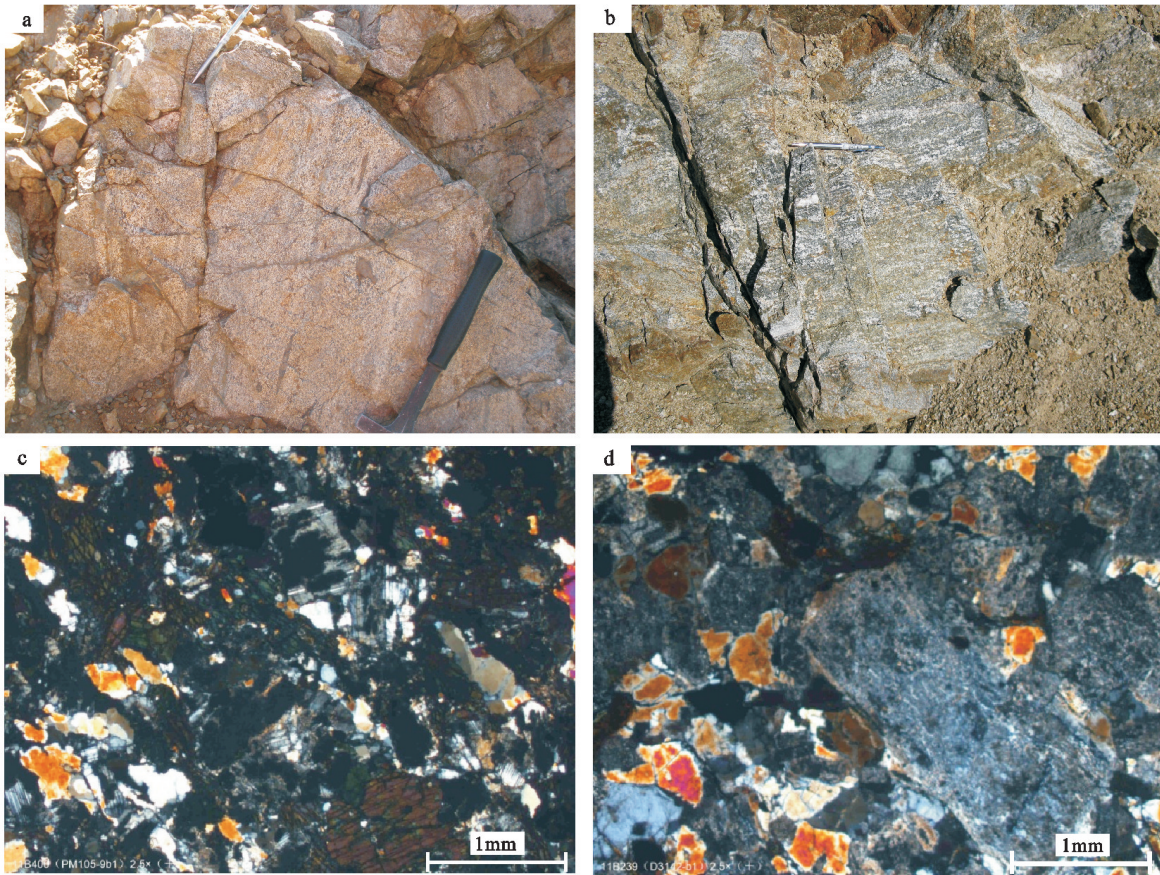


图2 石英闪长岩野外与显微照片

Fig.2 Representative field photos and photomicrographs of quartz diorites

显示了岩浆成因的特征^[21]。样品 D3014-TW1 的 25 个点的测试结果 U 含量和 Th/U 比值分别为 104×10^{-6} ~ 572×10^{-6} 和 0.31×10^{-6} ~ 0.73×10^{-6} ; 样品 D3021-TW1 的 23 个点的测试结果 U 含量和 Th/U 比值分别为 65×10^{-6} ~ 246×10^{-6} 和 0.34×10^{-6} ~ 0.68×10^{-6} ; 均反映了岩浆成因的特征。D3014-TW1 和 D3021-TW1 的 $^{206}\text{Pb}/^{238}\text{U}$ 年龄加权平均值分别为 (304.64 ± 0.82) Ma (MSWD = 0.71) 和 (309.84 ± 0.86) Ma (MSWD = 0.40) (图 4), 代表了石英闪长岩的侵位结晶年龄。

4 地球化学特征

石英闪长岩的主量元素和微量元素分析结果见表 2。

4.1 主量元素

石英闪长岩的 SiO_2 质量分数为 58.22% ~ 62.68%; Al_2O_3 含量较高 (15.69% ~ 17.27%), 平均 16.21%; MgO 含量偏低 (2.76% ~ 4.08%), $\text{Mg}^\#$ 为

47.1~52.56; TiO_2 质量分数比较低 (0.59%~0.80%), 平均 0.69%; Na_2O 和 K_2O 含量分别为 2.85%~3.86%、1.24%~2.01%, $\text{Na}_2\text{O}/\text{K}_2\text{O}$ 比值 1.58~3.10, 为钠质岩石; 铝饱和指数 A/CNK 值介于 0.88~1.08, 平均 0.98, 属于准铝质及弱的过铝质。在 TAS 图解中 (图 5-a) 所有样品均分布在亚碱性闪长岩区域, 并且里特曼指数 σ 为 1.23~1.68, 属钙性岩石, 与 TAS 图解结果相符。AFM 图解中 (图 5-b) 样品落入钙碱性玄武岩系列范围。

4.2 微量元素

安第斯活动大陆边缘弧玄武岩 Nb 含量为 5.3×10^{-6} , Ta 为 0.25×10^{-6} ~ 0.5×10^{-6} , Ni 为 38.6×10^{-6} , Cr 为 48.4×10^{-6} ; 而岛弧钙碱性玄武岩 Nb 含量为 0.7×10^{-6} , Ta 为 0.1×10^{-6} , Ni 为 50×10^{-6} , Cr 为 160×10^{-6} [22]。研究区石英闪长岩 Nb 的含量为 3.05×10^{-6} ~ 4.33×10^{-6} , Ta 为 0.28×10^{-6} ~ 0.42×10^{-6} (除样品 D3014 异常 1.55×10^{-6}), Ni 为 9.03×10^{-6} ~ 18.4×10^{-6} , Cr 为 18.4×10^{-6} ~

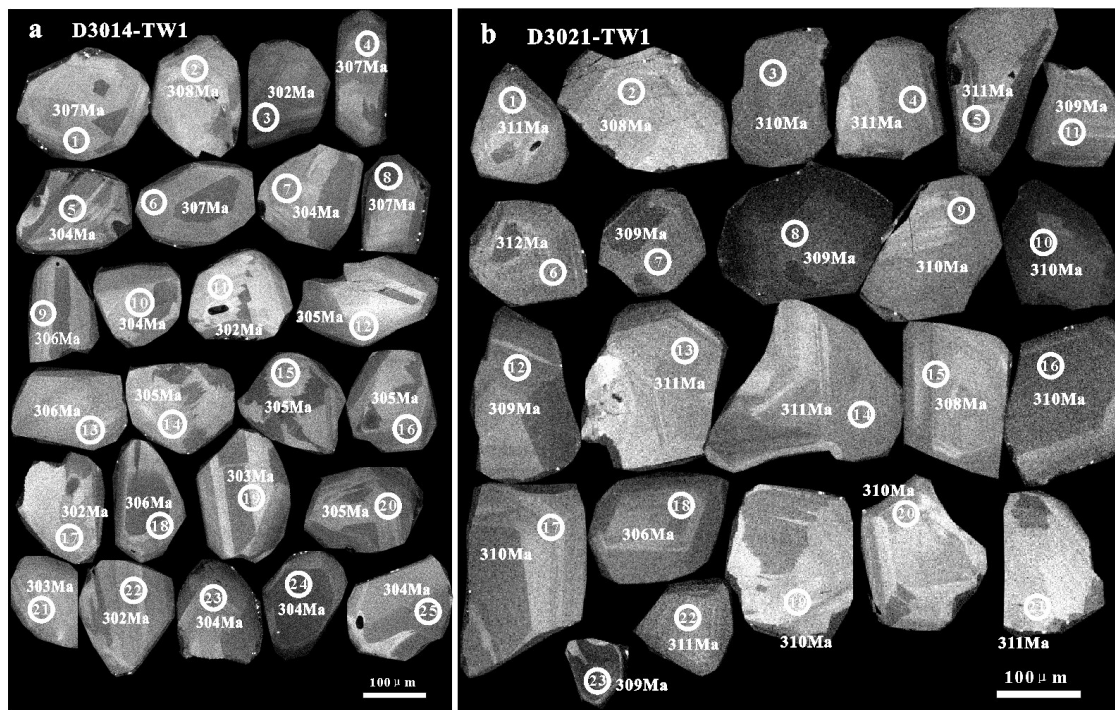


图3 石英闪长岩锆石阴极发光图像

Fig. 3 CL images for analyzed zircon grains from quartz diorites

51.4×10^{-6} , 总体与安第斯活动大陆边缘弧玄武岩接近。在原始地幔标准化的微量元素比值蛛网图中(图6-a), 同样显示LILE和Th富集和Nb、Ta、Ti、P等高场强元素的亏损, 与弧岩浆岩微量元素分布型式相似^[23], 同样具有与俯冲作用有关岩浆岩的特征^[24]。

4.3 稀土元素

石英闪长岩稀土总量为 $82.27 \times 10^{-6} \sim 100.68 \times 10^{-6}$, $(La/Yb)_N$ 为 2.79~3.92 ($LREE/HREE=1.46 \sim 1.85$), 具有弱的负Eu异常, δEu 为 0.74~0.94。轻稀土元素内部存在明显的分馏作用 ($(La/Sm)_N=1.57 \sim 2.16$), 而重稀土元素内部存在较弱的分馏作用 ($(Gd/Yb)_N=1.07 \sim 1.46$)。球粒陨石标准化的REE曲线(图6-b)呈LREE富集HREE亏损的右倾模式。

5 讨论

5.1 岩石成因

高场强元素如Nb、Ta、Ti等在蚀变和变质作用过程中具有良好稳定性, 是岩石成因和源区性质的良好示踪剂。源于软流圈地幔的玄武岩 $La/Nb < 1.5$, $La/Ta < 22$, 岩石圈地幔玄武岩则与之相反^[25]。研究区石英闪长岩的 La/Nb 为 2.45~3.40, La/Ta 为

25.44~37.10(样品D3014比较低, 为6.96), 说明本区岩石来源于岩石圈地幔。一般地壳岩石的 TiO_2 含量很低(平均0.72%^[26]), 来自软流圈的岩浆 TiO_2 含量在1.27%左右^[23], 而与深部地幔物质活动有关的岩浆, TiO_2 含量往往大于2.0%^[27]。测区晚石炭世石英闪长岩 TiO_2 质量分数为0.59%~0.80%, 平均值为0.69%, TiO_2 含量较低, 显示岩浆源区主要与浅部的地幔有关。

一般地, 当尖晶石二辉橄榄岩发生部分熔融时, 地幔残留体和熔体具有相似的Sm/Yb比值, 而La/Sm比值将随着部分熔融程度的增高而降低, 因此, 尖晶石二辉橄榄岩源区的部分熔融将产生相对水平的熔融趋势(接近或靠近地幔排列); 而石榴石二辉橄榄岩源区(源区残留有石榴石)中低程度部分熔融产生的熔体具有显著增高的Sm/Yb比值, 导致石榴石二辉橄榄岩的熔融趋势明显偏离地幔排列^[27-28]。在Sm/Yb-La/Sm图(图7-a)上, 研究区石英闪长岩投点与石榴石+尖晶石二辉橄榄岩熔融趋势为代表的地幔排列趋势一致, 暗示岩浆主要来源于石榴石+尖晶石二辉橄榄岩源区中等程度(10%~20%)的部分熔融。Dy/Yb也是判断源区性质的重

表1 西乌旗地区石英闪长岩 LA-ICP-MS 锆石 U-Pb 测年结果
 Table 1 LA-ICP-MS zircon U-Pb isotopic data of quartz diorites from Xi Ujimqin Banner

| 测点号 | 含量/ 10^{-6} | | $^{232}\text{Th}/^{238}\text{U}$ | 同位素比值 | | | | | | 表面年龄/Ma | | | |
|----------|---------------|-----|----------------------------------|----------------------------------|-----------|----------------------------------|-----------|-----------------------------------|-----------|----------------------------------|-----------|----------------------------------|-----------|
| | Pb | U | | $^{206}\text{Pb}/^{238}\text{U}$ | 1σ | $^{207}\text{Pb}/^{235}\text{U}$ | 1σ | $^{207}\text{Pb}/^{206}\text{Pb}$ | 1σ | $^{206}\text{Pb}/^{238}\text{U}$ | 1σ | $^{207}\text{Pb}/^{235}\text{U}$ | 1σ |
| D3014-1 | 9 | 165 | 0.52 | 0.0488 | 0.0004 | 0.3558 | 0.0158 | 0.0529 | 0.0024 | 307 | 2 | 309 | 14 |
| D3014-2 | 7 | 132 | 0.50 | 0.049 | 0.0004 | 0.3554 | 0.0224 | 0.0526 | 0.0033 | 308 | 3 | 309 | 19 |
| D3014-3 | 5 | 104 | 0.45 | 0.048 | 0.0004 | 0.3518 | 0.0175 | 0.0532 | 0.0026 | 302 | 3 | 306 | 15 |
| D3014-4 | 6 | 112 | 0.31 | 0.0488 | 0.0004 | 0.3541 | 0.0081 | 0.0527 | 0.0012 | 307 | 2 | 308 | 7 |
| D3014-5 | 14 | 266 | 0.44 | 0.0483 | 0.0003 | 0.3576 | 0.0117 | 0.0536 | 0.0017 | 304 | 2 | 310 | 10 |
| D3014-6 | 10 | 174 | 0.69 | 0.0488 | 0.0003 | 0.356 | 0.0099 | 0.0529 | 0.0015 | 307 | 2 | 309 | 9 |
| D3014-7 | 20 | 376 | 0.62 | 0.0482 | 0.0003 | 0.3574 | 0.0099 | 0.0538 | 0.0015 | 304 | 2 | 310 | 9 |
| D3014-8 | 10 | 192 | 0.45 | 0.0488 | 0.0003 | 0.3559 | 0.0109 | 0.0529 | 0.0016 | 307 | 2 | 309 | 9 |
| D3014-9 | 11 | 195 | 0.71 | 0.0486 | 0.0003 | 0.3525 | 0.0105 | 0.0526 | 0.0016 | 306 | 2 | 307 | 9 |
| D3014-10 | 9 | 160 | 0.73 | 0.0483 | 0.0003 | 0.3519 | 0.0101 | 0.0528 | 0.0015 | 304 | 2 | 306 | 9 |
| D3014-11 | 13 | 250 | 0.60 | 0.048 | 0.0003 | 0.3507 | 0.0161 | 0.053 | 0.0024 | 302 | 2 | 305 | 14 |
| D3014-12 | 11 | 206 | 0.45 | 0.0485 | 0.0003 | 0.3542 | 0.0136 | 0.053 | 0.002 | 305 | 2 | 308 | 12 |
| D3014-13 | 29 | 572 | 0.41 | 0.0485 | 0.0003 | 0.358 | 0.0126 | 0.0535 | 0.0018 | 306 | 2 | 311 | 11 |
| D3014-14 | 6 | 123 | 0.48 | 0.0485 | 0.0003 | 0.358 | 0.0115 | 0.0535 | 0.0017 | 305 | 2 | 311 | 10 |
| D3014-15 | 12 | 240 | 0.37 | 0.0484 | 0.0003 | 0.3514 | 0.0116 | 0.0527 | 0.0017 | 305 | 2 | 306 | 10 |
| D3014-16 | 11 | 196 | 0.59 | 0.0485 | 0.0003 | 0.3499 | 0.013 | 0.0523 | 0.0019 | 305 | 2 | 305 | 11 |
| D3014-17 | 14 | 258 | 0.57 | 0.048 | 0.0003 | 0.3514 | 0.0115 | 0.0532 | 0.0017 | 302 | 2 | 306 | 10 |
| D3014-18 | 10 | 180 | 0.52 | 0.0487 | 0.0003 | 0.3526 | 0.0153 | 0.0525 | 0.0023 | 306 | 2 | 307 | 13 |
| D3014-19 | 11 | 209 | 0.63 | 0.0481 | 0.0003 | 0.3504 | 0.0133 | 0.0528 | 0.002 | 303 | 2 | 305 | 12 |
| D3014-20 | 9 | 154 | 0.67 | 0.0485 | 0.0003 | 0.3547 | 0.0149 | 0.0531 | 0.0021 | 305 | 2 | 308 | 13 |
| D3014-21 | 8 | 157 | 0.36 | 0.0482 | 0.0003 | 0.357 | 0.0127 | 0.0537 | 0.0019 | 303 | 2 | 310 | 11 |
| D3014-22 | 8 | 156 | 0.43 | 0.0479 | 0.0003 | 0.347 | 0.01 | 0.0525 | 0.0015 | 302 | 2 | 302 | 9 |
| D3014-23 | 10 | 191 | 0.47 | 0.0483 | 0.0003 | 0.3571 | 0.01 | 0.0536 | 0.0015 | 304 | 2 | 310 | 9 |
| D3014-24 | 18 | 354 | 0.45 | 0.0483 | 0.0003 | 0.3589 | 0.0071 | 0.0539 | 0.0011 | 304 | 2 | 311 | 6 |
| D3014-25 | 11 | 204 | 0.64 | 0.0483 | 0.0003 | 0.3497 | 0.0114 | 0.0525 | 0.0017 | 304 | 2 | 305 | 10 |
| D3021-1 | 6 | 107 | 0.4164 | 0.0494 | 0.0003 | 0.3694 | 0.0116 | 0.0543 | 0.0017 | 311 | 2 | 319 | 10 |
| D3021-2 | 6 | 102 | 0.5494 | 0.0489 | 0.0003 | 0.522 | 0.0116 | 0.0774 | 0.0016 | 308 | 2 | 425 | 9 |
| D3021-3 | 8 | 151 | 0.4027 | 0.0493 | 0.0003 | 0.3686 | 0.0075 | 0.0542 | 0.0011 | 310 | 2 | 319 | 7 |
| D3021-4 | 5 | 101 | 0.3445 | 0.0495 | 0.0003 | 0.3584 | 0.0121 | 0.0525 | 0.0017 | 311 | 2 | 311 | 10 |
| D3021-5 | 7 | 124 | 0.4208 | 0.0494 | 0.0003 | 0.3652 | 0.0098 | 0.0536 | 0.0014 | 311 | 2 | 316 | 9 |
| D3021-6 | 6 | 107 | 0.4277 | 0.0496 | 0.0003 | 0.3635 | 0.0117 | 0.0532 | 0.0017 | 312 | 2 | 315 | 10 |
| D3021-7 | 5 | 106 | 0.4043 | 0.0491 | 0.0003 | 0.372 | 0.0105 | 0.0549 | 0.0015 | 309 | 2 | 321 | 9 |
| D3021-8 | 7 | 130 | 0.4711 | 0.0491 | 0.0003 | 0.3556 | 0.0089 | 0.0525 | 0.0013 | 309 | 2 | 309 | 8 |
| D3021-9 | 12 | 246 | 0.3402 | 0.0492 | 0.0003 | 0.3615 | 0.0049 | 0.0532 | 0.0007 | 310 | 2 | 313 | 4 |
| D3021-10 | 5 | 102 | 0.4167 | 0.0493 | 0.0003 | 0.3684 | 0.0113 | 0.0542 | 0.0016 | 310 | 2 | 318 | 10 |
| D3021-11 | 11 | 224 | 0.3416 | 0.0491 | 0.0003 | 0.3653 | 0.0062 | 0.054 | 0.0009 | 309 | 2 | 316 | 5 |
| D3021-12 | 5 | 91 | 0.4193 | 0.0491 | 0.0003 | 0.3635 | 0.0127 | 0.0537 | 0.0018 | 309 | 2 | 315 | 11 |
| D3021-13 | 7 | 135 | 0.5738 | 0.0494 | 0.0003 | 0.3815 | 0.0089 | 0.056 | 0.0013 | 311 | 2 | 328 | 8 |
| D3021-14 | 5 | 84 | 0.4655 | 0.0494 | 0.0003 | 0.3746 | 0.0123 | 0.055 | 0.0018 | 311 | 2 | 323 | 11 |
| D3021-15 | 6 | 109 | 0.4122 | 0.049 | 0.0004 | 0.3596 | 0.0138 | 0.0532 | 0.0017 | 308 | 2 | 312 | 12 |
| D3021-16 | 6 | 117 | 0.4262 | 0.0493 | 0.0003 | 0.3836 | 0.0095 | 0.0564 | 0.0014 | 310 | 2 | 330 | 8 |
| D3021-17 | 9 | 171 | 0.5827 | 0.0493 | 0.0003 | 0.3855 | 0.0076 | 0.0567 | 0.0011 | 310 | 2 | 331 | 6 |
| D3021-18 | 3 | 54 | 0.3689 | 0.0486 | 0.0004 | 0.3559 | 0.0189 | 0.0531 | 0.0028 | 306 | 2 | 309 | 16 |
| D3021-19 | 4 | 77 | 0.4988 | 0.0493 | 0.0003 | 0.3787 | 0.0183 | 0.0557 | 0.0026 | 310 | 2 | 326 | 16 |
| D3021-20 | 6 | 104 | 0.6805 | 0.0492 | 0.0003 | 0.3707 | 0.0146 | 0.0546 | 0.0021 | 310 | 2 | 320 | 13 |
| D3021-21 | 4 | 81 | 0.571 | 0.0494 | 0.0003 | 0.3645 | 0.0133 | 0.0535 | 0.0019 | 311 | 2 | 316 | 11 |
| D3021-22 | 3 | 65 | 0.5273 | 0.0495 | 0.0003 | 0.3725 | 0.0177 | 0.0546 | 0.0026 | 311 | 2 | 322 | 15 |
| D3021-23 | 4 | 75 | 0.5036 | 0.049 | 0.0004 | 0.3691 | 0.0153 | 0.0546 | 0.0023 | 309 | 2 | 319 | 13 |

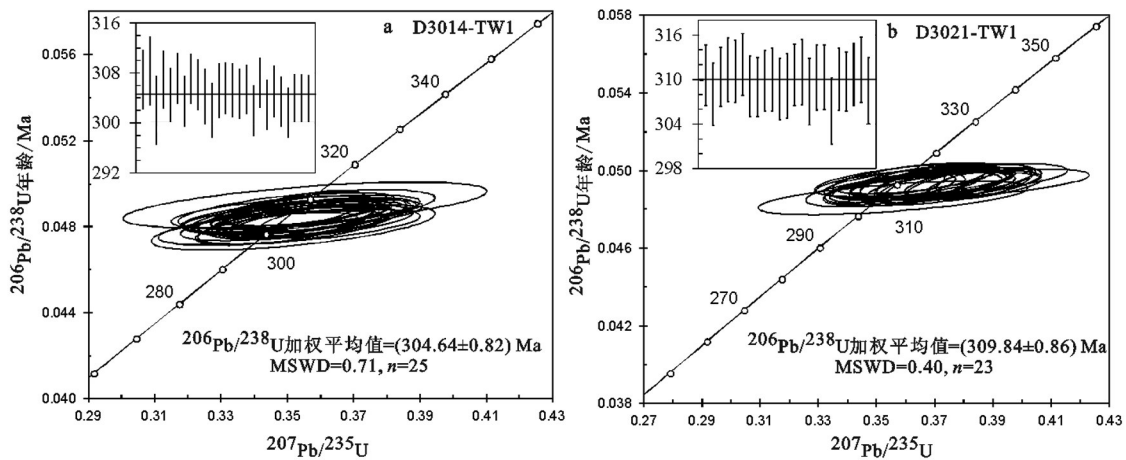


图4 石英闪长岩LA-ICP-MS锆石U-Pb年龄协和图

Fig. 4 LA-ICP-MS U-Pb concordia diagrams for analyzed zircon grains from quartz diorites

要指标;如果源区是石榴石稳定区域,其熔体的Dy/Yb > 2.5;如果熔融作用在尖晶石稳定区域,则熔体的Dy/Yb < 1.5^[29]。研究区石英闪长岩Dy/Yb为1.72~2.06,比值介于石榴石稳定区与尖晶石稳定区之间,也说明其岩浆为石榴石+尖晶石二辉橄榄岩部分熔融的产物。

岩石明显富集LILE(K、Rb、Ba)、LREE和强不相容元素Th,亏损Nb、Ta、P、Ti等高场强元素,具有岛弧或活动大陆边缘弧岩浆岩的特点。岩石具有明显的“TNT”(Ta、Nb、Ti)异常,Sun and McDonough^[23]认为其主要为俯冲带幔源岩石的特点。在图La/Nb-La/Ba中(图7-b),所有样品位于俯冲改造的大陆岩石圈区域,再次证明源区主要受到消减带流体交代作用的影响。在Ba/La-Ce/Pb图解(图8-a)中,样品分布在沉积岩与俯冲带岩浆区域内,暗示源区在部分熔融之前可能经历了沉积物质的影响^[31]。Nb/Y和La/Nb比值图解(图8-b)更进一步说明源区主要受俯冲板块流体交代作用控制^[32]。

5.2 构造环境

一些强不相容元素对在岩浆活动中由于其分配系数远小于部分熔融比例,并且在变质过程中具有较好的稳定性,其比值在部分熔融及分离结晶过程中保持不变,从而可以消除岩石后期变化及岩浆演化过程中的影响,反映原始岩浆及源区的性质^[33-34],因此可以作为判断其形成的构造环境及源区性质的依据。表3列出了研究区不相容元素的元素对比值。

严格按照Condie^[33]提出的不同构造背景玄武岩的判别流程,发现本区石英闪长岩属于大陆边缘弧钙碱性玄武岩(CABC)。

在Nb×2-Zr/4-Y三角图解(图9-a)中,所有样品落入C和D区域,表明这些样品不是板内碱性玄武岩和富集洋中脊玄武岩,但是难以进一步区分这些样品是正常洋中脊玄武岩、板内拉斑玄武岩还是火山弧玄武岩。已有研究表明,Hf/3-Th-Nb/16构造环境判别图解可以识别出洋中脊玄武岩、板内碱性玄武岩以及火山弧拉斑玄武岩^[35],Hf/3-Th-Nb/16图解(图9-b)表明这些样品为火山弧玄武岩。另外,Canbanis and Lecolle^[36]提出的Y/15-La/10-Nb/8图解(图9-c)可以用来区分火山弧玄武岩、大陆玄武岩和大洋玄武岩,该图解判别结果表明,所有样品落入钙碱性大陆火山弧玄武岩及过渡区域。并且在区分大洋弧还是大陆边缘弧的Th/Yb-Ta/Yb图解(图9-d)中,样品基本投影在大陆边缘弧区域及附近,而未落入板内玄武岩和洋中脊玄武岩区域,进一步辅助Nb×2-Zr/4-Y三角图解证明样品为火山弧玄武岩。

因此,上述一系列玄武岩构造环境判别图解及微量元素比值均表明研究区石英闪长岩具有大陆边缘弧玄武岩的特征。

5.3 构造意义

西乌旗地区石英闪长岩的LA-ICP-MS锆石U-Pb年龄分别为(304.6±0.82)Ma和(309.8±0.86)

表2 西乌旗地区石英闪长岩主量元素分析结果(%)、微量元素分析结果(10^{-6})Table 2 Major (%) and trace element (10^{-6}) analytical result of quartz diorites from Xi Ujimqin Banner

| 样号 | PM105-1YQ1 | PM105-15YQ1 | D3021YQ1 | PM003-25YQ1 | PM003-26YQ1 | D3014YQ1 |
|----------------------------------|------------|-------------|----------|-------------|-------------|----------|
| SiO ₂ | 58.78 | 58.71 | 59.78 | 58.49 | 62.68 | 58.22 |
| Al ₂ O ₃ | 16.06 | 15.92 | 16.09 | 17.27 | 15.69 | 16.21 |
| TiO ₂ | 0.72 | 0.70 | 0.64 | 0.67 | 0.59 | 0.80 |
| Fe ₂ O ₃ | 2.40 | 2.73 | 2.39 | 3.41 | 3.03 | 2.64 |
| FeO | 4.44 | 4.19 | 4.17 | 3.14 | 2.59 | 4.74 |
| CaO | 6.25 | 5.87 | 5.33 | 4.76 | 3.65 | 5.89 |
| MgO | 3.65 | 4.08 | 3.89 | 3.07 | 2.76 | 3.92 |
| K ₂ O | 1.89 | 1.73 | 1.39 | 1.24 | 2.01 | 1.39 |
| Na ₂ O | 2.98 | 2.85 | 3.28 | 3.86 | 3.49 | 2.95 |
| MnO | 0.13 | 0.12 | 0.13 | 0.11 | 0.11 | 0.13 |
| P ₂ O ₅ | 0.12 | 0.15 | 0.13 | 0.13 | 0.11 | 0.17 |
| LOI | 2.48 | 2.86 | 2.48 | 3.74 | 3.22 | 2.81 |
| TOTAL | 99.90 | 99.89 | 99.68 | 99.89 | 99.91 | 99.85 |
| A/CNK | 0.88 | 0.92 | 0.97 | 1.06 | 1.08 | 0.95 |
| A/NK | 2.31 | 2.43 | 2.33 | 2.25 | 1.98 | 2.55 |
| σ | 1.50 | 1.33 | 1.30 | 1.68 | 1.53 | 1.23 |
| Mg [#] | 49.87 | 52.46 | 52.56 | 47.10 | 48.30 | 49.76 |
| V | 152.28 | 167.20 | 147.20 | 150.93 | 143.37 | 132.70 |
| Cr | 34.87 | 51.40 | 26.44 | 23.95 | 27.67 | 18.40 |
| Co | 20.53 | 21.60 | 16.72 | 17.96 | 17.06 | 15.93 |
| Ni | 14.07 | 18.40 | 13.54 | 13.57 | 13.95 | 9.03 |
| Cu | 45.08 | 34.40 | 37.11 | 130.70 | 36.13 | 73.90 |
| Zn | 64.59 | 66.40 | 65.86 | 64.79 | 62.79 | 60.56 |
| Ga | 15.70 | 15.72 | 13.85 | 15.64 | 16.15 | 11.74 |
| Rb | 56.76 | 54.70 | 39.35 | 41.67 | 73.47 | 35.39 |
| Sr | 298.02 | 322.50 | 273.20 | 400.90 | 319.01 | 205.10 |
| Zr | 131.50 | 113.20 | 62.50 | 106.90 | 134.60 | 43.61 |
| Nb | 4.19 | 3.71 | 3.05 | 3.66 | 4.33 | 3.96 |
| Cs | 1.06 | 1.29 | 1.70 | 1.48 | 2.05 | 1.16 |
| Ba | 233.60 | 281.00 | 133.60 | 142.10 | 250.20 | 147.40 |
| Hf | 6.72 | 6.03 | 0.96 | 5.48 | 6.75 | 0.64 |
| Ta | 0.40 | 0.37 | 0.28 | 0.33 | 0.42 | 1.55 |
| Pb | 9.60 | 8.40 | 8.61 | 7.72 | 9.64 | 7.85 |
| Th | 5.23 | 4.95 | 4.57 | 10.00 | 11.19 | 3.04 |
| U | 1.34 | 1.34 | 0.73 | 0.96 | 1.20 | 0.83 |
| La | 11.68 | 11.86 | 10.35 | 11.20 | 10.61 | 10.81 |
| Ce | 25.93 | 25.33 | 25.29 | 24.58 | 22.25 | 24.96 |
| Pr | 3.56 | 3.53 | 3.43 | 3.52 | 3.13 | 3.30 |
| Nd | 15.85 | 15.62 | 15.57 | 16.31 | 13.48 | 14.07 |
| Sm | 3.84 | 3.80 | 4.13 | 4.20 | 3.09 | 3.47 |
| Eu | 1.12 | 1.08 | 0.92 | 1.05 | 0.82 | 1.00 |
| Gd | 3.63 | 3.54 | 3.53 | 4.00 | 2.81 | 3.09 |
| Tb | 0.71 | 0.68 | 0.72 | 0.78 | 0.54 | 0.62 |
| Dy | 4.16 | 4.19 | 4.52 | 4.54 | 3.21 | 3.99 |
| Ho | 0.93 | 0.91 | 0.90 | 0.98 | 0.69 | 0.79 |
| Er | 2.50 | 2.45 | 2.43 | 2.52 | 1.87 | 2.26 |
| Tm | 0.48 | 0.48 | 0.42 | 0.46 | 0.38 | 0.39 |
| Yb | 2.30 | 2.32 | 2.50 | 2.21 | 1.83 | 2.32 |
| Lu | 0.35 | 0.34 | 0.34 | 0.33 | 0.26 | 0.32 |
| Y | 21.35 | 21.70 | 25.63 | 22.97 | 17.32 | 22.11 |
| Σ REE | 98.40 | 97.83 | 100.68 | 99.64 | 82.27 | 93.50 |
| LREE/HRE | 1.70 | 1.67 | 1.46 | 1.57 | 1.85 | 1.61 |
| (La/Yb) _N | 3.42 | 3.45 | 2.79 | 3.42 | 3.92 | 3.14 |
| δ Eu | 0.92 | 0.90 | 0.74 | 0.78 | 0.85 | 0.94 |
| La _N /Sm _N | 1.91 | 1.96 | 1.57 | 1.68 | 2.16 | 1.96 |
| Gd _N /Yb _N | 1.27 | 1.23 | 1.14 | 1.46 | 1.24 | 1.07 |
| La/Nb | 2.79 | 3.20 | 3.40 | 3.06 | 2.45 | 2.73 |
| La/Ta | 29.05 | 32.05 | 37.10 | 33.73 | 25.44 | 6.96 |
| Dy/Yb | 1.81 | 1.81 | 1.81 | 2.06 | 1.76 | 1.72 |
| Nb/U | 3.12 | 2.77 | 4.17 | 3.82 | 3.60 | 4.79 |

Ma。锆石结晶较好,具有岩浆岩锆石的特征,因此锆石年龄代表了岩体的形成年龄。野外观测到晚石炭世本巴图组、阿木山组呈角度不整合覆盖于石英闪长岩体之上,这也验证了同位素年龄测定结果的正确性。两个石英闪长岩的形成年龄相近,并且在微量元素蛛网图和球粒陨石标准化分配图上所

有样品具有相似的曲线分布形式,表明两套岩体具有同源的特点。因此,西乌旗地区的石英闪长岩应该为同一期岩浆作用,岩浆活动时代为晚石炭世。

研究表明,中亚造山带形成于“多地体、多俯冲、多岛弧、多碰撞”的复杂构造背景,伴随着古亚洲洋的俯冲和闭合,产生了广泛的岛弧、蛇绿岩、增

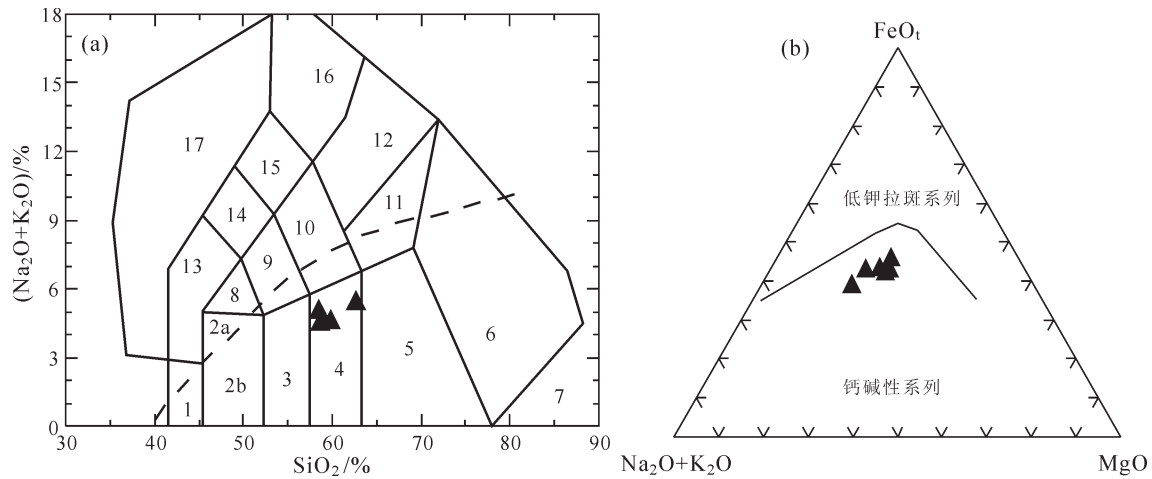


图5 TAS图解(a)和AFM图解(b) (据[22]修改)

1—橄榄辉长岩; 2a—碱性辉长岩; 2b—亚碱性辉长岩; 3—辉长闪长岩; 4—闪长岩; 5—花岗闪长岩; 6—花岗岩; 7—石英岩;
 8—二长辉长岩; 9—二长闪长岩; 10—二长岩; 11—石英二长岩; 12—正长岩; 13—副长石辉长岩; 14—副长石二长闪长岩;
 15—副长石二长正长岩; 16—副长正长岩; 17—副长深成岩虚线下方亚碱性, 上方碱性

Fig. 5 TAS diagram (a) and AFM diagram (b) (modified after reference [22])

1—Olive gabbro; 2a—Alkaline gabbro; 2b—Sub-alkaline gabbro; 3—Gabbro diorite; 4—Diorite; 5—Granodiorite; 6—Granite; 7—Quartzolite;
 8— Monzogabbro; 9—Monzodiorite; 10—Monzonite; 11—Quartz monzonite; 12—Syenite; 13—Foid gabbro; 14—Foid monzodiorite;
 15—Foid monzosyenite; 16— Foid syenite; 17—Foid plutonite The sub-alkaline rocks are below the dashed line, whereas the alkaline rocks are above the dashed line

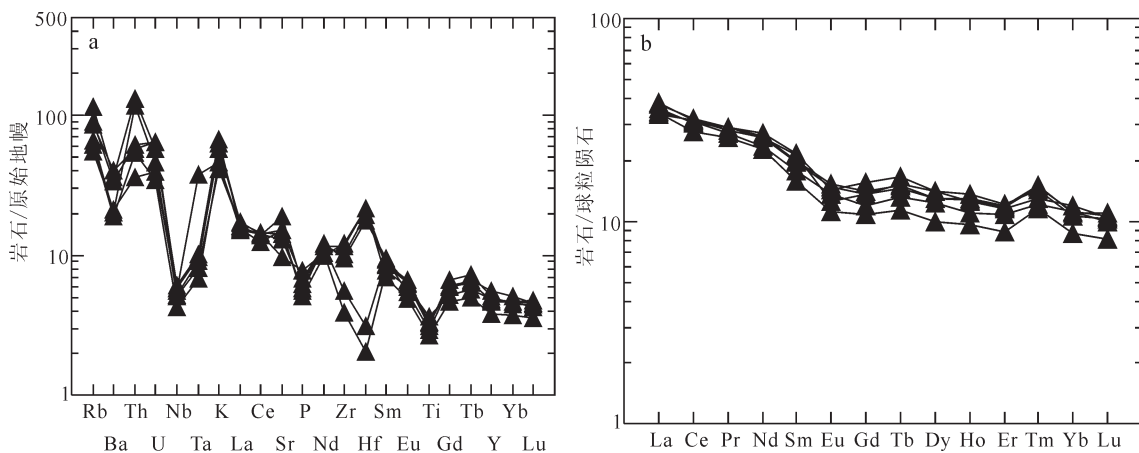


图6原始地幔标准化微量元素蛛网图(a)和稀土元素球粒陨石标准化图(b) (据[23])

Fig. 6 Primitive mantle-normalized trace elements spider diagram (a) and chondrite-normalized REE patterns (b) (modified after reference [23])

生楔和增生造山, 以及诸多微地块的碰撞造山作用, 形成了比较复杂的中亚造山带。晚古生代是兴蒙造山带乃至中亚构造演化的一个关键阶段, 古亚洲洋的闭合以及大规模的成矿作用均发生在这一时期^[3-5,39]。有关兴蒙造山带石炭纪的构造环境一直存在争议, 有些学者认为石炭纪古亚洲洋已经闭合,

发育陆表海和裂陷槽, 与造山后伸展作用有关^[8-10,13]; 有些学者提出石炭纪仍为俯冲的构造环境^[3-4,15,18]。兴蒙造山带石炭—二叠纪广泛发育裂谷活动^[40], 现在越来越多的资料说明石炭—二叠纪时本区广泛发育双峰式火山岩、碱性花岗岩和基性岩, 属于裂谷环境^[41-44], 与造山后阶段以发育巨量花岗岩和强烈岩

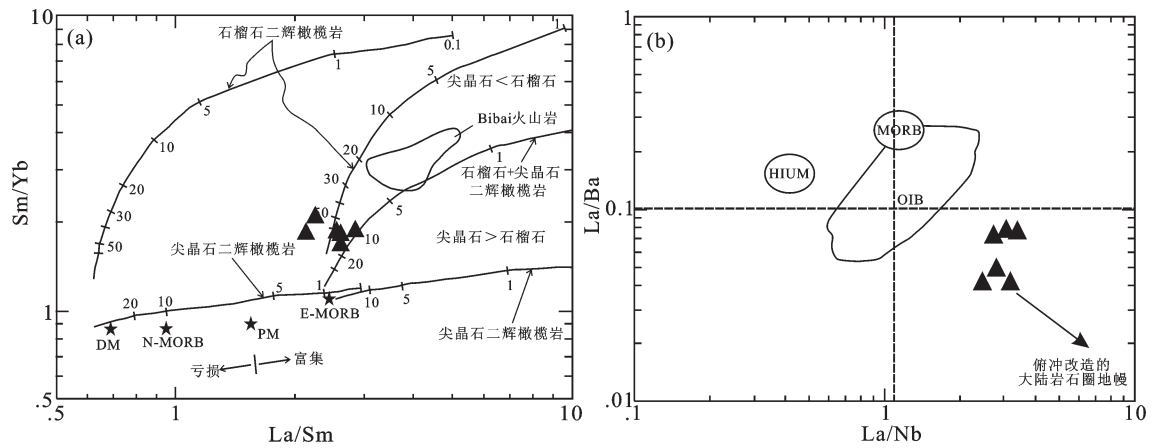


图7 Sm/Yb-La/Sm图解 (a,据[27]) 和 La/Nb-La/Ba图解 (b,据[30])

DM—亏损地幔;PM—原始地幔;N-MORB—正常洋中脊玄武岩;E-MORB—富集洋中脊玄武岩;MORB—洋中脊玄武岩;OIB—洋岛玄武岩;HIUM—高U/Pb比值地幔

Fig. 7 Sm/Yb-La/Sm diagram (a) (modified after reference [27]) and La/Nb-La/Ba diagram (b) (modified after reference [30])
DM-Depleted mantle; PM-Primitive mantle; N-MORB-Normal mid-ocean ridge basalts; E-MORB-Enriched mid-ocean ridge basalts; MORB-Mid-ocean ridge basalts; OIB-Ocean island basalts; HIUM-High U/Pb ratio mantle

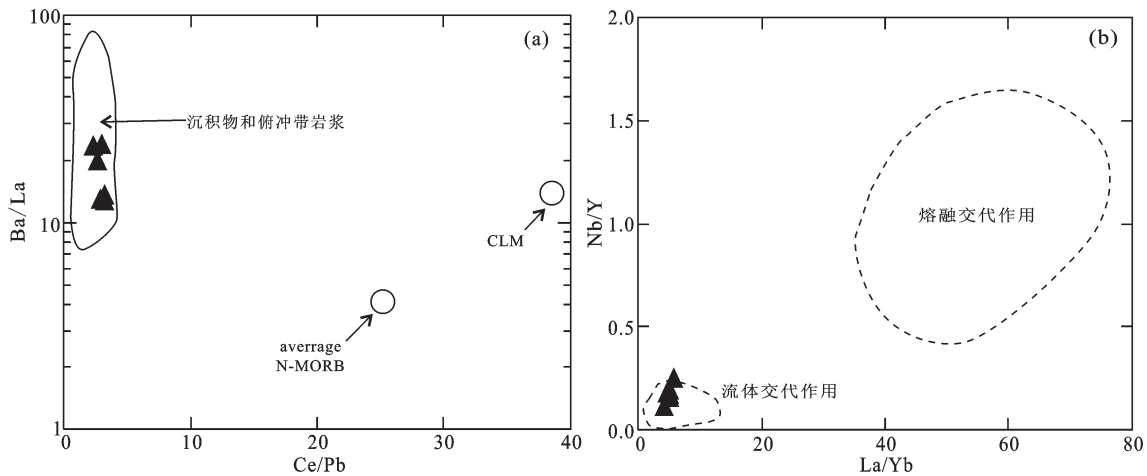


图8 Ce/Pb-Ba/La图解(a) (据[31])和 La/Yb-Nb/Y图解(b) (据[32])

average N-MORB—平均正常洋中脊玄武岩; CLM—大陆岩石圈地幔

Fig. 8 Ce/Pb-Ba/La diagram (a) (modified after reference [31]) and La/Yb-Nb/Y diagram (a) (modified after reference [32])
average N-MORB-Average mid-ocean ridge basalts; CLM-Continental lithospheric mantle

浆作用为标志的认识较为一致^[45-46]。西乌旗白音高勒地区的晚石炭世石英闪长岩形成于华北板块与亲西伯利亚板块碰撞之后的张性构造环境^[19];并且陈彦等^[43]认为西乌旗地区早二叠世双峰火山岩具有板内成因特征,形成于碰撞后的伸展环境。从地质特征来看,在东乌旗—西乌旗贺根山蛇绿岩带两侧,局部发育的上石炭统(格根敖包组)滨浅海碎屑

岩和碳酸盐岩中夹有大量安山岩、粗安岩和晶屑凝灰岩,反映拉伸减薄作用中地壳成熟度降低的过程^[47]。西乌旗地区石炭—二叠纪海槽同期异相地层、大石寨组双峰式火山岩^[48]和东乌旗晚石炭—早二叠世宝力高庙组陆相火山岩^[49],亦显示了区域伸展构造环境特征。

通过1:5万区域地质调查在该区新发现超基性

表3 西乌旗地区石英闪长岩不相容元素对比值判别构造环境

Table 3 Incompatible element ratios for discriminating tectonic environment of quartz diorites from Xi Ujimqin Banner

| 样号 | PM105-1YQ1 | PM105-15YQ1 | D3021YQ1 | PM003-25YQ1 | PM003-26YQ1 | D3014YQ1 | 平均值 |
|------------------|------------|-------------|----------|-------------|-------------|----------|--------|
| 第一级划分 | | | | | | | |
| Nb/La | 0.36 | 0.31 | 0.29 | 0.33 | 0.41 | 0.37 | 0.34 |
| Hf/Ta | 16.72 | 16.30 | 3.44 | 16.51 | 16.18 | 0.41 | 11.59 |
| La/Ta | 29.05 | 32.05 | 37.10 | 33.73 | 25.44 | 6.96 | 27.39 |
| Ti/Y | 201.63 | 194.50 | 149.49 | 175.92 | 202.53 | 216.48 | 190.09 |
| Ti/V | 28.27 | 25.24 | 26.03 | 26.77 | 24.46 | 36.07 | 27.81 |
| TiO ₂ | 0.72 | 0.70 | 0.64 | 0.67 | 0.59 | 0.80 | 0.69 |
| Ta | 0.40 | 0.37 | 0.28 | 0.33 | 0.42 | 1.55 | 0.56 |
| Nb | 4.19 | 3.71 | 3.05 | 3.66 | 4.33 | 3.96 | 3.82 |
| 第二级划分 | | | | | | | |
| Th/Yb | 2.27 | 2.13 | 1.83 | 4.53 | 6.12 | 1.31 | 3.03 |
| Th/Nb | 1.25 | 1.33 | 1.50 | 2.73 | 2.59 | 0.77 | 1.69 |
| Nb/La | 0.36 | 0.31 | 0.29 | 0.33 | 0.41 | 0.37 | 0.34 |
| Hf/Th | 1.29 | 1.22 | 0.21 | 0.55 | 0.60 | 0.21 | 0.68 |
| 第三级划分 | | | | | | | |
| Zr/Y | 6.16 | 5.22 | 2.44 | 4.65 | 7.77 | 1.97 | 4.70 |
| Ta/Yb | 0.17 | 0.16 | 0.11 | 0.15 | 0.23 | 0.67 | 0.25 |

岩、基性岩,地球化学特征同李英杰^[50-51]新发现内蒙古西乌旗迪彦庙蛇绿岩相似,可能为本区的洋壳残片^[52]。白卉^[53]对西乌旗迪彦庙蛇绿岩中的辉长岩进行LA-ICP-MS 锆石U-Pb测年,获得年龄为(320±1)Ma,与本区辉长岩锆石年龄(321±2Ma)吻合,说明早石炭世末期本区在强烈拉张的环境下形成了裂隙槽,并且在地壳相对较薄或者裂隙较深的部位,可能形成了尚未成熟的新洋盆^[54]。在早二叠世时期,满都拉所处的索伦—贺根山一带在强烈拉张的裂谷背景下进一步发育成有限洋盆^[55]。通过对贺根山两侧西乌旗和东乌旗地区晚石炭世岩体的研究,虽然大部分岩体被划为后碰撞伸展构造环境的产物^[19,43,47,56-57],但少数岩体具有火山弧的特征^[11,58-59]。而且本文的石英闪长岩也具有俯冲带弧岩浆岩的地球化学特征。因此,在综合分析和对比的基础上,结合前人的研究成果,本文认为在早石炭世末—早二叠世时期,贺根山一带处于强烈的裂谷背景下,并且在强烈拉张的环境下逐步形成了新洋盆。其中西乌旗地区洋盆形成于早石炭世末期,由于洋盆发育不成熟或边伸展边向两侧俯冲—消减,导致浅部地幔部分熔融形成了本区具有大陆边缘弧特征

的晚石炭世石英闪长岩。

6 结 论

(1)西乌旗地区石英闪长岩LA-ICP-MS 锆石U-Pb 年龄分别为(304.64±0.82)Ma 和(309.84±0.86)Ma,属于晚石炭世。

(2)西乌旗地区晚石炭世石英闪长岩富集Rb、Ba、K 大离子亲石元素和强不相容元素Th,亏损Nb、Ta、Ti、P 等高场强元素,具有火山弧玄武岩的特征,显示岩浆源区受到过消减带流体的交代作用;同时TiO₂含量较低(平均0.69%),强不相容元素比值(La/Nb > 1.5, La/Ta > 22, 等)及图解,指示其岩浆来源于浅部的岩石圈地幔,系石榴石+尖晶石二辉橄榄岩源区中等程度(10%~20%)部分熔融的结果。

(3)综合研究区样品的地球化学特征、结合区域地质资料以及对比分析前人研究成果,认为早石炭世末期西乌旗地区在强烈拉张的裂谷环境下形成了有限洋盆,由于洋盆发育不成熟或边伸展边向两侧俯冲—消减,导致浅部地幔部分熔融形成了本区具有大陆边缘弧特征的晚石炭世石英闪长岩。

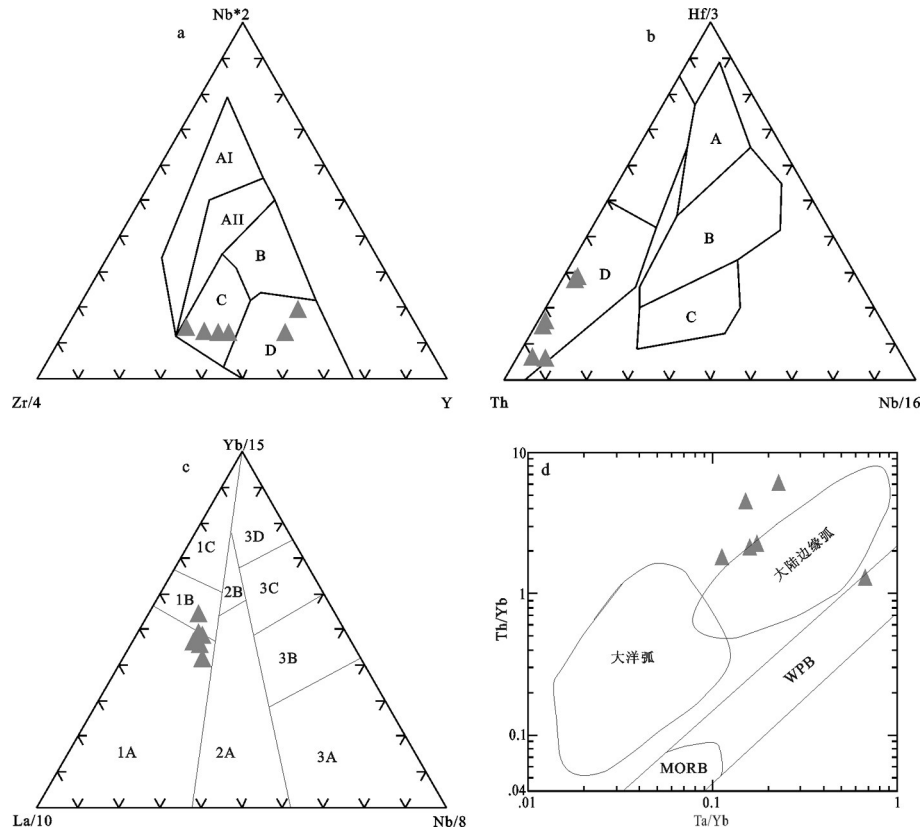


图9 微量元素构造环境判别图解(据[35-38])

- a: A I + A II—板内碱性玄武岩; B—富集型洋中脊玄武岩; C—板内拉斑玄武岩+火山弧玄武岩; D—正常洋中脊玄武岩+火山弧玄武岩。
 b: A—正常洋中脊玄武岩; B—富集型洋中脊玄武岩; C—板内碱性玄武岩及分异产物; D—火山弧拉斑玄武岩及分异产物。
 c: 1A—钙碱性大陆火山弧玄武岩; 1B—钙碱性大陆火山弧玄武岩和大陆火山弧拉斑玄武岩区过渡区; 1C—大陆火山弧拉斑玄武岩区; 2A—大陆玄武岩; 2B—弧后盆地玄武岩; 3A—大陆裂谷碱性玄武岩; 3B和3C—异常洋中脊玄武岩; 3D—正常洋中脊玄武岩。
 d: MORB—洋中脊玄武岩; WPB—板内玄武岩

Fig. 9 Tectonic environmental discriminative diagrams of trace elements(modified after references [35-38])

(Fig. a. modified after reference [37]; Fig. b. modified after reference [35]; Fig. c. modified after reference [36]; Fig. d. modified after reference [38])

- a: A I + A II—Intraplate alkali basalts; B, E—MORB, Enriched mid-ocean ridge basalts; C, Intraplate tholeiites and volcanic-arc basalts; D—N—MORB and volcanic-arc basalts. b: A—N—MORB, Normal mid-ocean ridge basalts; B—E—MORB, Enriched mid-ocean ridge basalts; C—Intraplate alkaline basalts; D—Island-arc tholeiites. c: 1A—Calcium alkaline continental island arc basalts; 1B—Transition zone; 1C—Volcanic arc tholeiite; 2A—Continental basalts; 2B—Arc-back basin basalts; 3A—Continental rift alkaline basalts; 3B and 3C, Abnormal mid-ocean ridge basalts; 3D—Normal mid-ocean ridge basalts. d: MORB—Mid-ocean ridge basalts; WPB—Intraplate basalt

致谢:野外得到高德臻教授、张能高工、刘志慧博士、杜杨工程师的的指导与帮助,行文过程中得到李宝霞工程师的帮助,审稿专家和编辑部老师为论文的最终定稿付出了大量心血,对他们的帮助一并表示衷心感谢。

参考文献(References):

[1] 王荃, 刘雪亚, 李锦轶. 中国内蒙古中部的古板块构造[M]. 北京: 北京大学出版社, 1991, 1-151
 Wang Quan, Liu Xueya, Li Jinyi. Plate Tectonics between

Cathaysia and Angaraland in China[M]. Beijing: Peking University Press, 1991, 1-151(in Chinese).

[2] Tang Kedong. Tectonic development of Paleozoic fold belts at the north margin of the Sino-Korean craton[J]. Tectonics, 1990, 9(2): 249-260.
 [3] Xiao W J, Windley B F, Hao J, et al. Accretion leading to collision and the Permian Solonker suture, Inner Mongolia, China: Termination of the central Asian orogenic belt[J]. Tectonics, 2003, 22(6): 1069-1089.
 [4] Li J Y. Permian geodynamic setting of Northeast China and adjacent regions: closure of the Paleo-Asian Ocean and subduction of the Paleo-Pacific Plate[J]. Journal of Asian Earth Sciences,

- 2006, 26(3-4): 207-224.
- [5] Windley B F, Alexeiev D, Xiao W J, et al. Tectonic models for accretion of the Central Asian Orogenic Belt[J]. *Journal of the Geological Society*, 2007, 164(1): 31-47.
- [6] 洪大卫, 黄怀曾, 肖宜君, 等. 内蒙中部二叠纪碱性花岗岩及其地球动力学意义[J]. *地质学报*, 1994, 68(3): 219-230.
Hong Dawei, Huang huazeng, Xiao Yijun, et al. The Permian Alkaline Granites in Central Inner Mongolia and their geodynamic significance.[J]. *Acta Geologica Sinica*, 1994, 68(3): 219-230 (in Chinese with English abstract).
- [7] 徐备, 陈斌. 内蒙古北部华北板块与西伯利亚板块之间中生代造山带的结构及演化[J]. *中国科学D辑*, 1997, 27(3): 227-232.
Xu Bei., Chen Bin. The structure and evolution of Paleozoic orogenic belt between the north China plate of the northern Inner Mongolia and Siberian plate[J]. *Science in China (Series D)*, 1997, 27(3): 227-232 (in Chinese).
- [8] 徐备, 赵盼, 鲍庆中, 等. 兴蒙造山带前中生代构造单元划分初探[J]. *岩石学报*, 2014, 30(7): 1841-1857.
Xu Bei, Zhao Pan, Bao Qingzhong, et al. Preliminary study on the pre-Mesozoic tectonic unit division of the Xing-Meng Orogenic Belt (XMOB) [J]. *Acta Petrologica Sinica*, 2014, 30(7): 1841-1857 (in Chinese with English abstract).
- [9] 邵济安. 中朝板块北缘中段地壳演化[M]. 北京: 北京大学出版社, 1991: 1-136.
Shao Ji'an. Crust Evolution in the Middle part of the Northern Margin of Sino-Korean Plate[M]. Beijing: Peking University Press, 1991: 1-136 (in Chinese).
- [10] 邵济安, 唐克东, 何国琦. 内蒙古早二叠世构造古地理的再造[J]. *岩石学报*, 2014, 30(7): 1858-1866.
Shao Jian, Tang Kedong, He Guoqi. Early Permian tectono-palaeogeographic reconstruction of Inner Mongolia, China[J]. *Acta Petrologica Sinica*, 2014, 30(7): 1858-1866 (in Chinese with English abstract).
- [11] 刘建峰, 迟效国, 张兴洲, 等. 内蒙古西乌旗南部石炭纪石英闪长岩地球化学特征及其构造意义[J]. *地质学报*, 2009, 83(3): 365-376.
Liu Jianfeng, Chi Xiaoguo, Zhang Xingzhou, et al. Geochemical Characteristics of Carboniferous Quartz-Diorite in the Southern Xiwuqi Area, Inner Mongolia and Its Tectonic Significance[J]. *Acta Geologica Sinica*, 2009, 83 (3): 365-376 (in Chinese with English abstract).
- [12] 唐克东, 张允平. 内蒙古缝合带的构造演化[M]//肖序常, 汤耀庆主编. 古中亚复合巨型缝合带南缘构造演化. 北京: 北京科学技术出版社, 1991, 30-54.
Tang Kedong, Zhang Yunping. Tectonic Evolution of Inner Mongolian Suture Zone[M]//Xiao Xuchang, Tang Yaoqing(eds.). Tectonic Evolution of the southern margin of the Paleo-Asian composite Megasuture. Beijing: Beijing Scientific and Technical House, 1991: 30-54 (in Chinese).
- [13] 曹从周, 杨芳林, 田昌裂, 等. 内蒙古贺根山地区蛇绿岩和中朝板块和西伯利亚板块之间的缝合带位置[C]//中国北方板块构造论文集, 第1集, 北京: 地质出版社, 1986: 64-86.
Cao Congzhou, Yang Fanglin, Tian Changlie et al. The ophiolite in Hegenshan district, Nei Mongol and the Position of Suture Line between Sino-Korean and Siberian plates[C]//Proceedings of north China plate tectonics, 1 set. Beijing: Geological Publishing House, 1986: 64-86 (in Chinese).
- [14] Sengor A M C, Natal'in B A, Burtman V S. Evolution of the Altaid tectonic collage and Paleozoic crustal growth in Eurasia[J]. *Nature*, 1993, 364 (22): 299-307.
- [15] Chen Bin, Jahn Bor-ming, Wilde S, et al. Two contrasting Paleozoic magmatic belts in northern Inner Mongolia, China: Petrogenesis and tectonic implications[J]. *Tectonophysics*, 2000, 328(1-2): 157-182.
- [16] 陈斌, 赵国春, Simon Wilde. 内蒙古苏尼特左旗南两类花岗岩同位素年代学及其构造意义[J]. *地质论评*, 2001, 47(4): 361-367.
Chen Bin, Zhao Guochun, Simon Wilde. Subduction- and Collision-related Granitoids from Southern Sonidzuoqi, Inner Mongolia: Isotopic Ages and Tectonic Implications[J]. *Geological Review*, 2001, 47(4): 361-367 (in Chinese with English abstract).
- [17] Miao L C, Fan W M, Liu D Y, et al. Geochronology and geochemistry of the Hegenshan ophiolitic complex: implications for late-stage tectonic evolution of the Inner Mongolia-Daxinganling Orogenic Belt[J]. *Journal of Asian Earth Sciences*, 2008, 32(5/6): 348-370.
- [18] Xiao W J, Windley B F, Huang B C, et al. End-Permian to Mid-Triassic Termination of the accretionary processes of the southern Altaids: Implications for the geodynamic evolution, Phanerozoic continental growth, and metallogeny of Central Asia[J]. *International Journal of Earth Science*, 2009, 98(6): 1219-1220.
- [19] 鲍庆中, 张长捷, 吴之理, 等. 内蒙古白音高勒地区石炭纪石英闪长岩 SHRIMP 锆石 U-Pb 年代学及其意义[J]. *吉林大学学报(地球科学版)*, 2007, 37(1): 15-23.
Bao Qingzhong, Zhang Changjie, Wu Zhili, et al. SHRIMP U-Pb zircon geochronology of a Carboniferous quartz-diorite in Baiyingaole area, Inner Mongolia and its implications[J]. *Journal of Jilin University (Earth Science Edition)*, 2007, 37(1): 15-23 (in Chinese with English abstract).
- [20] 李怀坤, 朱士兴, 相振群, 等. 北京延庆高于庄组凝灰岩的锆石 U-Pb 定年研究及其对华北北部中元古界划分新方案的进一步约束[J]. *岩石学报*, 2010, 26(7): 2131-2140.
Li Huaikun, Zhu Shixing, Xiang Zhenqun, et al. Zircon U-Pb dating on tuff bed from Gaoyuzhuang Formation in Yangqing, Beijing: Further constrains on the new subdivision of the Mesoproterozoic stratigraphy in the northern North Chian Craton[J]. *Acta Petrologica Sinica*, 2010, 26 (7): 2131-2140 (in Chinese with English abstract).
- [21] Wu Yuanbao, Zheng Yongfei. Genesis of zircon and its constraints on interpretation of U-Pb age[J]. *Chinese Science Bulletin*, 2004, 49(15): 1554-1569.
- [22] Wilson M. Igneous Petrogenesis: A Global Tectonic

- Approach[M]. Unwin Hyman, London, 1989, 1-466.
- [23] Sun S S, McDonough W F. Chemical and isotope systematics of oceanic basalts: implications for mantle composition and process. In: *Magmatism in ocean Basins* (Saunders, AD) (eds.) [M]. Geological Society, London, Special Publications, 1989, 42: 313-345.
- [24] Altherr R, Topuz G, Sicbel W, et al. Geochemical and Sr-Nd-Pb isotopic characteristics of Paleocene plagioclinites from the eastern Pontides (NE Turkey) [J]. *Lithos*, 2008, 105 (1/2): 149-161.
- [25] Huang Y M, Hawkesworth C, Smith I, et al. Geochemistry of Late Cenozoic basaltic volcanism in North land and Coromandel New Zealand Implications formantle enrichment processes[J]. *Chemical Geology*, 2000, 164(3-4): 219-238.
- [26] Rudnick R L, Gao S. Composition of the Continental Crust[C]// Holland H D, Turekian K K (eds.). *Treatise on Geochemistry*. Oxford, Elsevier, 2003: 1-51.
- [27] 朱弟成, 莫宣学, 王立全, 等. 新特提斯演化的热点与洋脊相互作用: 西藏南部晚侏罗世—早白垩世岩浆作用推论[J]. *岩石学报*, 2008, 24(2): 225-237.
- Zhu Dicheng, Mo Xuanxue, Wang Liqian, et al. Hotspot-ridge interaction for the evolution of Neo-Tethys: insights from the Late Jurassic—Early Cretaceous magmatism in southern Tibet[J]. *Acta Petrologica Sinica*, 2008, 24 (2): 225-237 (in Chinese with English abstract).
- [28] Aldanmaz E, Pearce J A, Thirlwall M F, et al. Petrogenetic evolution of late Cenozoic, post-collision volcanism in western Anatolia, Turkey[J]. *Journal of volcanology and geothermal research*, 2000, 102(1/2):67-95.
- [29] Jiang Y H, Jiang S Y, Dai B Z, et al. Middle to Late Jurassic felsic and mafic magmatism in southern Hunan Province, southeast China: Implications for a continental arc to rifting[J]. *Lithos*, 2009, 107(3/4): 185-204.
- [30] Saunders A D, Storey M, Kent R W, et al. Consequences of plume-lithosphere interactions[C]//Storey B C, Alabaster T, Pankhurst R J (eds.). *Magmatism and the Cause of Continental Breakup*. Geological Society, London, Special Publications, 1992, 68: 41-60.
- [31] Rottura A, Bargossi G M, Caggianelli A, et al. Origin and significance of the Permian high-K calc-alkaline magmatism in the central-eastern Southern Alps, Italy[J]. *Lithos*, 1998, 45(1-4):329-348.
- [32] Hoffer G, Eissen J P, Beate B, et al. Geochemical and petrological constrains on rear-arc magma genesis processes in Ecuador: The Puyo cones and Mera lavas volcanic formation[J]. *Journal of Volcanology and Geothermal Research*, 2008, 176(1): 107-118.
- [33] Condie K C. Geochemical changes in basalts and andesites across the Archaean-Proterozoic boundary: identification and significance[J]. *Lithos*, 1989, 23(1/2): 1-18
- [34] Hofmann A W. Mantle Geochemistry: The message from oceanic volcanism[J]. *Nature*, 1997, 385: 219-229.
- [35] Wood D A. The application of a Th-Hf-Ta diagram to problems of tectonomagmatic classification and to establishing the nature of crustal contamination of basaltic lavas of the British Tertiary volcanic province[J]. *Earth and Planetary Science Letters*, 1980, 50:11-30.
- [36] Cabanis B, Lecolle M. Le diagramme La/10-Y/15-Nb/8: Unoutil pour la discrimination de series volcaniques et la mise en evidence des processus de mélange et/ou de contamination crustale[J]. *Comptes Rendus Academie Sciences, Series II*, 1989, 309(20): 2023-2029.
- [37] Meschede M. A method of discriminating between different types of mid-ocean ridge basalts and continental tholeiites with the Nb-Zr-Y diagram[J]. *Chemical Geology*, 1986, 56: 207-218.
- [38] Pearce, J A. Trace element characteristics of lavas from destructive plate boundaries[C]//Thorps R S, Andesites (ed.). Chichester, Wiley: 1982: 525-548.
- [39] 蔡克大, 袁超, 孙敏, 等. 阿尔泰塔尔浪地区斜长角闪岩和辉长岩的形成时代、地球化学特征和构造意义[J]. *岩石学报*, 2007, 23 (5): 877-888
- Cai Keda, Yuan Chao, Sun Min, et al. Geochemical characteristics and $^{40}\text{Ar}-^{39}\text{Ar}$ ages of the amphibolites and gabbros in Tarlang area: implications for tectonic evolution of the Chinese Altai[J]. *Acta Petrologica Sinica*, 2007, 23 (5): 877-888 (in Chinese with English abstract).
- [40] 唐克东. 中朝陆台北侧褶皱带构造发展的几个问题[J]. *现代地质*, 1989, 3(2): 195-204.
- Tang Kedong. On tectonic development of the fold belts in the north margin of Sino-Korean platform[J]. *Geoscience*, 1989, 3 (2): 195-204 (in Chinese with English abstract).
- [41] 汤文豪, 张志诚, 李建峰, 等. 内蒙古苏尼特右旗查干诺尔石炭系本巴图组火山岩地球化学特征及其意义[J]. *北京大学学报(自然科学版)*, 2011, 47(2): 321-330.
- Tang Wenhao, Zhang Zhicheng, Li Jianfeng, et al. Geochemistry of the Carboniferous volcanic rocks of Benbatu Formation in Sonid Youqi, Inner Mongolia and its geological significance[J]. *Acta Scientiarum Naturalium Universitatis Pekinensis*, 2011, 47 (2): 321-330 (in Chinese with English abstract).
- [42] Yarmolyuk V V, Kovalenko V I, Sal'nikova E B, et al. Geochronology of igneous rocks and formation the Late Paleozoic South Mongolia active margin of the Siberian continent[J]. *Stratigraphy and Geological Correlation*, 2008, 16(2): 162-181.
- [43] 陈彦, 张志诚, 李可, 等. 内蒙古西乌旗地区二叠纪双峰式火山岩的年代学、地球化学特征和地质意义[J]. *北京大学学报(自然科学版)*, 2014, 50(5): 843-858.
- Chen Yan, Zhang Zhicheng, Li Ke, et al. Geochronology, Geochemistry and Geological Significance of the Permian Bimodal Volcanic Rocks in Xi Ujimqin Banner, Inner Mongolia[J]. *Acta Scientiarum Naturalium Universitatis Pekinensis*, 2014, 50(5): 843-858 (in Chinese with English abstract).

- abstract).
- [44] Cheng Yinhang, Teng Xuejian, Li Yanfeng, et al. Early Permian East-Ujimqin mafic-ultrafic and graniticrocks from the Xing'an-Mongolian Orogenic Belt, North China: Origin, chronology, and tectonic implications[J]. *Journal of Asian Earth Sciences*, 2014, 96: 361-373.
- [45] Liegeois L. P. Preface—Some words on the post-collisional magmatism[J]. *Lithos*, 1998, 45(1-4): xv-xvii.
- [46] 张旗, 钱青, 王焰. 造山带火成岩地球化学研究[J]. *地质前缘*, 1999, 6(3): 113-120.
Zhang Qi, Qian Qing, Wang Yan. Geochemical study on igneous rocks of orogenic belts[J]. *Earth Science Frontiers (China University of Geosciences, Beijing)*, 1999, 6(3): 113-120 (in Chinese with English abstract).
- [47] 梁玉伟, 余存林, 沈国珍, 等. 内蒙古东乌旗索纳嘎铅锌银矿区花岗岩地球化学特征及其构造与成矿意义[J]. *中国地质*, 2013, 40(3):767-780.
Liang Yuwei, Yu Cunlin, Shen Guozhen, et al. Geochemical characteristics of granites in the Suonaga Pb-Zn-Ag deposit of Dong Ujimqin Banner, Inner Mongolia, and their tectonic and ore-forming implications[J]. *Geology in China*, 2013, 40(3):767-780 (in Chinese with English abstract).
- [48] 鲍庆中, 张长捷, 吴之理, 等. 内蒙古东南部西乌珠穆沁旗地区石炭纪一二叠纪岩石地层和层序地层[J]. *地质通报*, 2006, 25(5): 572-579.
Bao Qingzhong, Zhang Changjie, Wu Zhili, et al. Carboniferous-Permian marine lithostratigraphy and sequence stratigraphy in Xi Ujimqin Qi, southeastern Inner Mongolia, China[J]. *Geological Bulletin of China*, 2006, 25(5): 572-579 (in Chinese with English abstract).
- [49] 辛后田, 滕学建, 程银行. 内蒙古东乌旗宝力高庙组地层划分及其同位素年代学研究[J]. *地质调查与研究*, 2011, 34(1): 1-9.
Xin Houtian, Teng Xuejian, Cheng Yinhang. Stratigraphic Subdivision and Isotope Geochronology Study on the Baoligaomiao Formation in the East Ujimqin County, Inner Mongolia[J]. *Geological Survey and Research*, 2011, 34(1): 1-9 (in Chinese with English abstract).
- [50] 李英杰, 王金芳, 李红阳, 等. 内蒙古西乌旗白音布拉格蛇绿岩地球化学特征[J]. *岩石学报*, 2013, 29(8): 2719-2730.
Li Yingjie, Wang Jinfang, Li Hongyang, et al. Geochemical characteristics of Baiyinbulage ophiolite in Xi Ujimqin Banner, Inner Mongolia[J]. *Acta Petrologica Sinica*, 2013, 29(8): 2719-2730(in Chinese with English abstract).
- [51] 李英杰, 王金芳, 李红阳, 等. 内蒙古西乌旗穆沁旗迪彦庙蛇绿岩的识别[J]. *岩石学报*, 2012, 28(4): 1282-1290.
Li Yingjie, Wang Jinfang, Li Hongyang, et al. Recognition of Diyanmiao ophiolite in Xi Ujimqin Banner, Inner Mongolia[J]. *Acta Petrologica Sinica*, 2012, 28(4): 1281-1290 (in Chinese with English abstract).
- [52] 董金元. 内蒙古西乌旗达青牧场蛇绿混杂岩特征及地质意义[D].北京:中国地质大学, 2014, 1-56.
Dong Jinyuan. Characteristics and Geological Significance of Ophiolite on the Area Daqingmuchang in Xiwuqi, Inner Mongolia[J]. Beijing: China University of Geosciences, 2014, 1-56 (in Chinese with English abstract).
- [53] 白卉. 内蒙古迪彦庙蛇绿岩地质地球化学特征[D]. 石家庄: 石家庄经济学院, 2013: 1-59.
Bai Hui. The Petrological and Geochemical Characteristics of Ophiolite on the Area of Diyanmiao in the Inner Mongolia[D]. Shijiazhuang: Shijiazhuang University of Economics, 2013: 1-59 (in Chinese with English abstract).
- [54] 苏养正. 内蒙古草原地层区的古生代地层[J]. *吉林地质*, 1996, (Z1): 42-54.
Su Yangzheng. Paleozoic Stratigraphy of Nei Mongol Grass Stratigraphical Pravice[J]. *Jilin Geology*, 1996, (Z1): 42-54 (in Chinese with English abstract).
- [55] Chen Chen, Zhang Zhicheng, Guo Zhaojie, et al. Geochronology, geochemistry, and its geological significance of the Permian Mandala mafic rocks in Damaoqi, Inner Mongolia[J]. *Sci China Earth Sci*, 2012, 55(1): 39-52.
- [56] 程银行, 滕学建, 辛后田, 等. 内蒙古东乌旗狼麦温都尔花岗岩 SHRIMP 锆石 U-Pb 年龄及其地质意义[J]. *岩石矿物学杂志*, 2012, 31(3): 323-334.
Cheng Yinhang, Teng Xuejian, Xin Houtian, et al. SHRIMP zircon U-Pb dating of granites in Mahonondor area, East Ujimqin Banner, Inner Mongolia[J]. *Acta Petrologica Et Mineralogica*, 2012, 31(3): 323-334 (in Chinese with English abstract).
- [57] 张玉清, 许立权, 康小龙, 等. 内蒙古东乌旗穆沁旗京格斯台碱性花岗岩年龄及意义[J]. *中国地质*, 2009, 36(5): 988-996.
Zhang Yuqing, Xu Liquan, Kang Xiaolong, et al. Age dating of alkali granite in Jingesitai area of Dong Ujimqin Banner, Inner Mongolia, and its significance [J]. *Geology In China*, 2009, 36(5): 988-996 (in Chinese with English abstract).
- [58] 贺宏云, 鞠文信, 宝音乌力吉. 内蒙古北部乌日尼图地区阿仁绍布辉长岩体的形成时代、地球化学特征及成因[J]. *沉积与特提斯地质*, 2011, 31(4): 70-78.
He Hongyun, Ju Wenxin, Baoyinwuliji. Age dating, geochemistry and petrogenesis of the Arenshaobu gabbro masses in the Wurinitu region, northern Inner Mongolia[J]. *Sedimentary Geology and Tethyan Geology*, 2011, 31(4): 70-78 (in Chinese with English abstract).
- [59] 云飞, 聂凤军, 江思宏, 等. 内蒙古莫若格钦地区二长闪长岩锆石 SHRIMP U-Pb 年龄及其地质意义[J]. *矿床地质*, 2011, 30(3): 504-510
Yun Fei, Nie Fengjun, Jiang Sihong, et al. Zircon SHRIMP U-Pb age of Monuogechin monzodiorite of Inner Mongolia and its geological significance[J]. *Mineral Deposits*, 2011, 30(3): 504-510 (in Chinese with English abstract).